# Potassium-induced effect on structure and chemical activity of $Cu_xO/Cu(111)$ ($x\leq2$) surface: a combined STM and DFT study

Wei An,[1,2] Fang Xu,[3] Dario Stacchiola[1] and Ping Liu[1,*]

[1]*Chemistry Department, Brookhaven National Laboratory, Upton, New York 11973, United States*

[2]*College of Chemistry and Chemical Engineering, Shanghai University of Engineering Science, Shanghai 201620, P.R. China*

[3] *Stony Brook University, Stony Brook, New York 11794, United States*

## Abstract

Potassium (K) plays an essential role in promoting catalytic reaction in many established industrial catalytic processes. Here, we report a combined study using scanning tunneling microscopy (STM) and density functional theory (DFT) in understanding the effect of depositing K on the atomic and electronic structures as well as chemical activities of $Cu_xO/Cu(111)$ ($x\leq2$). The DFT calculations observe a pseudomorphic growth of K on $Cu_xO/Cu(111)$ up to 0.19 monolayer (ML) of coverage, where K binds the surface via strong ionic interaction with chemisorbed oxygen and the relatively weak electrostatic interactions with copper ions, lower and upper oxygen on the $Cu_xO$ rings. The simulated STM pattern based on the DFT results agrees well with the experimental observations. The deposited K displays great impact on the surface electronic structure of $Cu_xO/Cu(111)$, which induces significant reduction in work function and leads to a strong electron polarization on the surface. The promotion of K on the surface binding properties is selective. It varies depending on the nature of adsorbates. According to our results, K has little effect on surface acidity, while it enhances the surface basicity significantly. As a consequence, the presence of K does not help for CO adsorption on $Cu_xO/Cu(111)$, but being able to accelerate the activation of $CO_2$. Such promotion strongly depends on the combinations from both geometric and electronic effects. Our results highlight the origin of promoting effect of alkalis in the design of catalysts for the complex reactions.

**Keywords**: Potassium; Electron polarization; $CO_2$; Copper oxide; DFT/STM

* Corresponding author E-mail: pingliu3@bnl.gov

## 1. Introduction

Potassium (K) plays an essential role in promoting catalytic reaction in many established industrial catalytic processes including water-gas-shift reaction, Haber-Bosch and Fischer-Tropsch processes.[1] It has been found that the incorporation of K not only greatly promotes the activity and selectivity of catalysts toward activation of various types of small molecules such as CO, $N_2$, $O_2$, NO, but also enhances the stability of catalysts under reaction conditions. Owing to its importance as a promoter, understanding the promoting effect of K has long been a subject in heterogeneous catalysis in both experiment[2] and theory[3] over the years. Several working mechanisms have been proposed, where both electronic and geometrical effects are evoked: (a) strengthening bindings via direct bonding with adsorbate,[3d] or electrostatic interactions (geometric effect);[3b] (b) modifying the electronic structure and therefore the activity of other active sites via electron transfers (electronic effect);[3h, 4] (c) reducing work function, which induces strong molecular polarization and surface electronic polarizability;[3g, 3i] (d) enhancing the stability of active sites on surfaces (geometric and electronic effects).[3f] Currently, there is no generally accepted picture, which hinders the deep understanding of the roles that K plays in tuning the catalytic performance of a catalyst. One of the obstacles is lacking of direct evidence on the location and distribution of K ions on the surface. The mechanisms proposed above were mainly based the theoretical studies using hypothetical models. The K-induced structural variation on catalyst surfaces still remains elusive.

In this contribution, we investigated the effects induced by deposing K on $Cu_xO$/Cu(111) ($x \leq 2$) surface using scanning tunneling microscopy (STM) and density functional theory (DFT). copper (Cu)-based catalysts have been reported active for many important reactions including water-gas-shift,[5] methanol or higher alcohol synthesis from $CO/CO_2$ hydrogenation,[6],[7] and CO oxidation.[8] K-promotion in the activity and selectivity of Cu-based systems are of special interests.[6c-k] To understand the promoting effect of K, extensive studies have been carried out on well-defined Cu surfaces as model systems.[6c-k, 9] However, under redox reaction conditions pure Cu cannot survive, but forming a Cu oxide thin film on the Cu surface even for practical metallic Cu powder catalysts.[10] Jensen et al.[11] and Matsumoto et al.[12] proposed that the structures of copper oxide films closely resembled $Cu_2O$ and existed in two forms known as the 29 and 44 structures. Both suggested that the 29 and 44 structures originated from the distortion of a $Cu_2O$(111)-like layer. The $Cu_2O$(111)-like film supported on Cu(111) has the same

hexagonal lattice as the unreconstructed $Cu_2O(111)$, but with the under-coordinated Cu atoms removed.[13] Therefore, such $Cu_xO/Cu(111)$ surface was used here as a model surface to simulate the Cu catalysts under reaction conditions.

In the present study, the combination of STM and DFT allows us to locate the position of K on the surface of $Cu_xO/Cu(111)$ readily, which provides a solid basis to identify the effect of K on the surface structures and chemical activities. Our DFT study observes a pseudomorphic growth of K on $Cu_xO/Cu(111)$ by occupying the chemisorbed oxygen sites at the center hexagonal $Cu_xO$ ring. The simulated STM pattern agrees well with the experimental observations. The distribution of electrons undergoes significant changes on depositing K, which results in the selective promotion in surface binding properties. The present study demonstrates the importance of combination of experiment and theory in understanding the complex surface structures and highlights the importance of K-induced electron polarization on the surface in tuning the catalytic performance of Cu-based catalysts.

## 2. Methods

### 2.1 Experimental method

All of the STM experiments were conducted in a SPECS™ Aarhus 150 HT STM chamber, with a background pressure of $5\times10^{-10}$ mbar. A Cu(111) single crystal (Princeton Scientific Corp.) was cleaned by cycles of sputtering (5 μA, 2.00 keV, 20 min, $Ar^+$) and annealing (850 Kelvin, 10 min). $Cu_xO/Cu(111)$ thin films were prepared by exposing the clean Cu(111) surface to $6\times10^{-7}$ mbar $O_2$ (GTS-WELCO, 99.999%) at elevated temperatures (550 - 650 Kelvin) for 20 min. A home-made potassium source was mounted normally to the $Cu_xO/Cu(111)$ surface for deposition purpose. All of the depositions were made at room temperature and the surfaces were post annealed under $6\times10^{-7}$ mbar $O_2$ at 500 Kelvin for 10 min to form flat terraces.

### 2.2 Theoretical method

Calculations were performed by using periodic DFT as implemented in the Vienna ab-initio simulation package (VASP).[14] Ion-core electron interactions were described using the projected augmented wave method (PAW).[15] Perdew-Wang functional (GGA-PW91) within the generalized gradient approximation (GGA)[16] was used to describe exchange-correlation effects, being able to well describe the experimentally observed electronic structure and chemical activity

of such system according to our previous studies.[13] The cutoff energy of plane-wave basis set was 400 eV. To model the 29/44-structure, we built a $Cu_xO$-like O-Cu-O overlayer on top of a three-layer *p*(4×4) Cu(111) slab. 9 Cu ions and 8 O ions were included in the oxide layer, which corresponds to 0.50 monolayer (ML) of oxygen coverage and x = 1.1 according to the ratio between Cu and O on the O-Cu-O layer. The obtained surface periodicity is 5.94 × 5.85Å, which closely matches experimental measurements of (6.1±0.1) × (5.9±0.1Å) and O-coverage of 0.52ML for 29/44-structure.[11-12] The two models are stable surface structures according to the previous study.[17] A vacuum of 20 Å between the slabs was applied perpendicular to the surface. The Brillouin-zone integration was sampled by 3×3×1 k-points, using the Monkhorst–Pack scheme,[18] The conjugate gradient algorithm was used in optimization, allowing the convergence of $10^{-4}$ eV in total energy and 0.02 eV/Å in Hellmann-Feynman force on each atom. All atoms were allowed to relax except those of the bottom two layers that were fixed at the bulk position with the optimized lattice constant of 3.63 Å.

The binding energy (BE) of an adsorbate (i.e., K, CO, $CO_2$) is defined as $BE = E_{A/slab} - E_{slab} - E_A$, where $E_{A/slab}$, $E_{slab}$, and $E_A$ is the total energy of an adsorbate adsorbed on $Cu_{1.1}O$/Cu(111), clean $Cu_{1.1}O$/Cu(111) slab, and the adsorbate in gas phase, respectively.

## 3. Results and Discussions

### 3.1 Atomic structure

The atomistic structures of $Cu_xO$-like thin film on Cu(111) have been the focus of STM studies.[11-13] The experimentally observed 44- and 29-structures are quite complex with long-range order rows and substructure of a hexagonal symmetry (6.1 ± 0.1 Å) × (5.9 ± 0.1 Å).[11] The 44-structure has a surface unit cell of (11.2 ± 0.1Å) × (21.9 ± 0.1 Å), 76.4° and 29-structure has a surface unit cell of (9.2 ± 0.1Å) × (18.0 ± 0.1 Å), 84.9°, where the surface unit cell can be schematically outlined by green lines in Figures 1a and 1b, respectively. So far, there is no generally accepted atomic structure to model the 44- and 29-structures mainly due to mismatch of symmetry and periodicity between the $Cu_xO$ ML film and Cu(111) substrate. In our DFT calculations, we employed $Cu_{1.1}O$/Cu(111) with 0.52 ML of oxygen coverage (Figures 1a and 1b) to describe $Cu_xO$/Cu(111) (blue lines, Figure 1), being able to well resemble that observed in our experimental STM images (Figures 1c and 1d) in terms of unit cell size and shape with reasonable computational cost. In addition, it is also able to captures the hexagonal

substructure features with similar lattice (5.9 × 5.8Å) compared to experiments (6.1 ± 0.1 Å × 5.9 ± 0.1 Å)[11] (white-dashed hexagon in Figure 1a and 1b). Unfortunately, our STM measurement can clearly distinguish the rings on the $Cu_2O$ structure, but the determination of occupied/unoccupied rings with chemisorbed oxygen is not straightforward. This model is among the most stable surface structures in terms of stability of chemisorbed oxygen[17] and have similar oxygen coverage with respect to the experiment. However, our model fails to capture the distorted angles with respect to Cu(111) substrate. To describe such a long-range surface reconstructions and distortions, a much larger supercell has to be employed in modeling, which is computationally too expensive.

We then investigated the effect of K on the structure of $Cu_xO$/Cu(111) using STM, where K was deposited on a $Cu_xO$/Cu(111) surface at 300 Kelvin. The surface is partially reduced and the deposited K binds to the surface with no diffusion. The images taken after deposition of K at 300 Kelvin can be used to estimate the coverage of K on the surface (inset, Figure 2a), assuming that one $Cu_2O$ hexagonal ring only contains one K atom. A sequential annealing of the K/$Cu_xO$/Cu(111) surface was performed in $5\times10^{-7}$ Torr $O_2$ at 500 K for 10 min, which led to the formation of a fully-oxidized surface with a K coverage of 0.12 ± 0.06 ML (Figure 2a). A nearly perfect hexagonal pattern is clearly formed with a unit cell of (9 ± 0.5) × (9 ± 0.5) $Å^2$, (62 ± 1)°. Unlike the buckled hexagonal network of $Cu_xO$(111)/Cu(111) due to the mismatch between the oxide film and the substrate, the hexagonal structure of the fully oxidized K/$Cu_xO$/Cu(111) surface is flat. Accordingly, we can correlate the isolated bright features with the presence of K on the $Cu_2O$(111) film, but the exact nature of the electronic perturbation of K on the oxide film is not known. K is imbedded in the $Cu_xO$ structure, and no local bright features are observed on the film.

In the DFT calculations, different adsorption sites on the $Cu_{1.1}O$/Cu(111) surface were considered for the nucleation sites of K: chemisorbed oxygen at the center of hexagon ring ($O_{ad}$), 3-coordinated upper oxygen ($O_U$), 4-coordinated lower oxygen ($O_L$)and $Cu^{\delta+}$ sites (Figure 1). Our results show that the K atom prefers to adsorb at the oxygen sites, while it desorbs from the $Cu^{\delta+}$ sites. The most stable adsorption site is the $O_{ad}$ site with the BE of -3.23 eV, which is followed by the $O_L$ site (BE = -2.75 eV) and the $O_U$ site (BE = -2.44 eV) in a decreasing sequence. Accordingly, to simulate the experimental annealing in oxygen-rich conditions, we saturated $Cu_{1.1}O$/Cu(111) with all hexagon rings filled with $O_{ad}$, which acts as a adsorption site

for K and transforms the surface to $Cu_{1.0}O/Cu(111)$ stoichiometry (Figure 2a). As such, a pseudomorphic growth of K with coverage of 0.19ML is obtained (Figure 2b), where the $O^{\delta-}$-$Cu^{\delta+}$-$O^{\delta-}$ hexagonal ring stays, but slightly changed in size and distorted in shape. The simulated STM shows a 10.3 Å × 10.3 Å 60.0° surface periodicity (Figure 2c), which is in good agreement with the STM measurement (Figure 2a) in consideration of the simplicity of our $Cu_{1.1}O/Cu(111)$ surface for $Cu_2O$-like thin film on Cu(111). On the basis of such agreement, we are able to assign the dark areas in the STM image of $K/Cu_{1.0}O/Cu(111)$ mainly to $O_L$, the big bright spots to K and the shaded areas to $O_U$ (Figure 2c). The deposition of K introduces the electron transfer to the surface together with the production of $K^{\delta+}$ on one hand; on the other hand it allows more $O_{ad}$ loaded on the surface, which is the preferential nucleation site for K on the $Cu_xO$ thin film. As a result, the further oxidation of the copper oxide film is observed due to the K deposition in oxygen atmosphere as will be demonstrated in Section 3.2.

The final arrangement of K on $Cu_{1.0}O/Cu(111)$ is mostly controlled by strong interaction with $O_{ad}$, where the K-$O_{ad}$ bond length is around 2.6 Å. It is similar to K-O bond length (2.8 Å) in $K_2O$ bulk, which indicates a direct ionic bonding. Besides, the relatively weak electrostatic interactions also exist between $K^+$ and $Cu^{\delta+}$ (repulsion with bond length of 3.1~3.5 Å) as well as $K^{\delta+}$ and $O_{U,L}^{\delta-}$ (attraction with bond length of 3~4 Å), which play a complementary role in determining the overlayer pattern of K-deposited $Cu_{1.0}O/Cu(111)$ (Figure 2b). That is, $K^{\delta+}$ can have geometrical effect on the morphology of a catalyst surface via direct bonding and direct electrostatic interactions, which has been previously observed by Jiao, et al.[3f]

### 3.2 Electronic structure

Figure 3a shows the calculated partial density of states (PDOS) of $O^{\delta-}$ before and after K deposition on $Cu_{1.1}O/Cu(111)$. Through the direct binding, K is able to stabilize the $O_{ad}$ sites. A downshift of O 2p is observed, while the shape remains almost the same (bottom panel in Figure 3a). In contrast, the effect on $O_U$ and $O_L$ is complex. In the case of $O_U$, the position of the 2p states stays the same before and after K deposition; yet it is redistributed with populated states around -5.2 eV (top panel in Figure 3a), which are associated with the electrostatic interaction with $K^{\delta+}$ as demonstrated in the PDOS of K 3p (arrow, bottom panel in Figure 3b). The K-induced variation in shape is also observed for the 2p state of $O_L$ (middle panel in Figure 3a); however, in this case the 2p states shift up towards the Fermi level, which likely indicates the

electron loss and therefore the activation of $O_L$. The calculated O-2p band center has been used as a descriptor for activity.[19] Accordingly, our calculated O 2p band centers ($O_U$: -4.83eV before K deposition and -5.06 eV after K deposition; $O_L$: -5.78eV before K deposition and -4.49eV after K deposition; $O_{ad}$: -4.19eV before K deposition and -4.36eV after K deposition) indicate the slight deactivation of $O_U$ and $O_{ad}$, but great enhancement in activation of $O_L$ as a result of K deposition.

The Cu 3d slightly splits after K deposition, where the additional states emerging at ~-5.2 eV seems associated with the electrostatic interaction with $K^{\delta+}$ (arrow, bottom panel in Figure 3b). In addition, the downshift of Cu 3d is also observed. It suggests that the further oxidation and therefore the enhanced stability of $Cu^{\delta+}$ on $Cu_{1.0}O/Cu(111)$, due to the additional oxygen introduced by K deposition. Overall, the electronic states of $O^{\delta-}$ are altered more pronounced than those of $Cu^{\delta+}$ as a result of K deposition. It implies that K has a major effect on the activity of $O^{\delta-}$ in terms of electron-donation capability (Lewis basicity), but a minor effect on $Cu^{\delta+}$ in terms of electron-acceptance (Lewis acidity).

There is a big difference in 3p states for the $K^{\delta+}$ supported on $Cu_{1.0}O/Cu(111)$ from the fully oxidized $K^+$ in bulk $K_2O$ (blue and red line, bottom panel in Figure 3b). The small occupied states for $K^+$ are very sharp and only located at -0.5 eV, where O 2p states are (green line, Figure 3b). In contrast, in the case of $K^{\delta+}$, they are broader and mainly localized at -5.2 eV, which overlaps with both Cu 3d (Figure 3b) and O 2p states ($O_{ad}$, $O_U$ and $O_L$, Figure 3a). This suggests that the nature of K-O bonds in $K/Cu_xO/Cu(111)$ surface structure is not a classical ionic bond as that in bulk $K_2O$, but rather a mixture of ionic bonding with small covalent features, as observed previously on both metal and oxide surfaces.[2g]

We also calculated the electron localization function (ELF) of $Cu_{1.1}O/Cu(111)$ before and after K deposition. The 2D slice of ELF projected above the surface was plotted (Figure 4). One can see that K has great impact on the landscape in electron density of $Cu_{1.0}O/Cu(111)$ surface. Before K deposition, the electron density is scarce and only localized at the sites over $O_U^{\delta-}$ (Figure 4a); while after the deposition the significant electron polarization over the surface is observed. More importantly, the effect is nonlocal, the substantial enhancement in electron density occurs not only over $K^{\delta+}$, but also over the entire surface area including $O_U^{\delta-}$ and $Cu^{\delta+}$ sites. Such alkali-induced surface electron polarization has been observed on metal surfaces.[3g, 3i] Differently from metal surfaces, $O_L$ at the subsurface of $Cu_{1.0}O/Cu(111)$ displays a K-induced

upshift in the 2p states towards the Fermi level (middle panel in Figure 3a), which indicates a activation of its valence electrons. Therefore a promotion of activity is expected. According to our previous study,[20] $O_{ad}$ is the most active oxygen species on the $Cu_xO/Cu(111)$ surface, followed sequentially by $O_L$ and $O_U$ in a decreasing sequence. However, $O_{ad}$ is not exposed to adsorbates because they are all covered and stabilized by K. As a result, $O_L$ is the most easily removed oxygen species in the hexagonal ring of $Cu_xO$ supported on Cu(111) and the high activity of $O_L$ can be further enhanced by depositing K.

Our findings of K-induced electron polarization over the $Cu_{1.1}O/Cu(111)$ surface (Figure 4) can be associated with the change in work function. The decreasing in work function from 5.3 eV to 2.0 eV upon K adsorption allows the electrons leak out further into the vacuum. The reduction in the work function arises from the dipole formation. The deposited K atoms easily form cationic species, which form an ionic overlayer with its valence electrons polarized towards the $Cu_{1.0}O/Cu(111)$ surface. It gives rise to a dipole barrier, which counteracts the original dipole for electron emission and thus reduces the work function.[21] Similar phenomenon is also observed for metal surfaces[2b] and metal supported oxide thin films: $Cr_2O_3(0001)/Cr(110)$,[22] $SiO_2/Mo(112)$, MgO/Ag(110) and $TiO_2/Pt(111)$.[23] Besides the alkalis, our previous studies also observed similar polarization effect by depositing Au particles on TiC(001), where such effect led to a flow of charge from the substrate to the supported particle and eventually promoted the catalytic properties of Au.[24]

### 3.3 Activity

We used CO and $CO_2$ as probe molecules to identify the effect of K deposition on the chemical activity of $Cu_xO/Cu(111)$. Activation of the CO and $CO_2$ molecule and the conversion into other compounds represents a grand challenge for catalysis.[6a] Since alkali promoters are able to negatively charge the molecule, the investigation of $CO/CO_2$ interaction with alkali metals is very promising for tailoring new catalysts for $CO_2$ sequestration.[2b] In addition, CO is known as a weak Lewis base which can be used to probe surface acidity of metal oxides, while $CO_2$ is a notable acidic molecule used for characterizing the Lewis basicity, independent of the surface acidity.[25] In general, stronger (weaker) binding means stronger (weaker) surface Lewis acidity (basicity) strength.[26]

According to our previous study,[20] CO prefers to adsorb at the atop site of $Cu^{\delta+}$ on $Cu_{1.1}O/Cu(111)$ with the BE of -0.47 eV. With the presence of K on the surface, the molecule favors the $Cu^{\delta+}$-$K^{\delta+}$ bridge site with the oxygen tilted towards $K^{\delta+}$ (Figure 5a), where the electrostatic interaction of $K^{\delta+}$ with O of CO is evidenced by 2.96 Å of K-O bond distance.[2j-l] However, the corresponding BE is only slightly increased by 0.02 eV in exothermicity, suggesting that K has little effect on CO activation. Both $Cu_{1.1}O/Cu(111)$ and $K/Cu_{1.0}O/Cu(111)$ surfaces are very weak Lewis acid. The adsorbed CO (*CO in our notation) has a slightly longer C-O bond length (1.17Å) on $K/Cu_{1.0}O/Cu(111)$ than that (1.15Å) on $Cu_{1.1}O/Cu(111)$, which suggests a K-induced red-shift in C-O stretch mode as observed on metal surfaces.[2j-l] This is supported by the calculated charge density difference (Figure 6a and b), where the charge depletion occurs at the C-O bond. In addition, the charge accumulation is mainly located around C and O ends of CO together with a small polarization in charge density of K, suggesting a weak activation toward CO by K deposition.

In contrast, K displays an enhancement in the surface basicity, being able to promote the $CO_2$ activation. The electrophilic properties of $CO_2$ lead to an expectation of charge transfer from the surface to the molecule to form an anion. One consequence of the degenerate ground state electronic structure of $*CO_2$ is that anion formation gives rise to changes in molecular geometry which tends to give "bent" chemisorbed species. As shown in Figure 5b, the O=C=O bond of $*CO_2$ is bent from the linear in gas-phase $CO_2$ to 145° with C and two O atoms interacting with $Cu^{\delta+}$ and $K^{\delta+}$ respectively; while without K it is only physisorbed and the molecule stays intact. That is, $*CO_2$ is chemisorbed (BE= -0.48 eV) and activated on $Cu_{1.0}O/Cu(111)$ due to the modification by K. The chemisorbed $*CO_2$ species is one of the key steps towards the activation of $CO_2$, which can either dissociate into CO and O, or dimerize to oxalate, or disproportionate to CO and carbonate.[3j, 6a, 27] Indeed, our calculations show that $K^{\delta+}$ is able to promote and stabilize the carbonate, $*CO_3$, species on $Cu_{1.1}O/Cu(111)$ (BE = -1.41eV, Figure 5c) more than $*CO_2$. Therefore, the conversion from $*CO_2$ to $*CO_3$ is likely to occur on $K/Cu_{1.0}O/Cu(111)$ under oxidizing conditions. One common feature for $*CO_2$ and $*CO_3$ is that K-O bond length is short enough to claim the direct bonding: 2.65 Å in adsorbed $*CO_2$, and 2.5~2.7Å in adsorbed $*CO_3$. It indicates that a strong ionic interaction is in play in promoting activation of $CO_2$. One can also see the direct K-O binding from the calculated PDOS. For

instance, the top panel in Figure 3b displays a strong overlapping in the DOS between the K and O of the adsorbed $CO_2$.

The promotion of K toward $CO_2$ activation is strongly associated with the K-induced electron polarization as demonstrated in Section 3.2. The polarized electron densities over $K^{\delta+}$ strongly attract the two O atoms of $CO_2$, and those over $Cu^{\delta-}$ help to adsorb the C atom of $CO_2$. As a result, the calculated charge density difference (Figure 6c and d) clearly shows that the charge accumulation is mainly located around two O ends of $CO_2$ and top of $Cu^{\delta+}$ which C of $CO_2$ binds; at mean time, charge depletion occurs at $O^{\delta-}$, or $K^{\delta+}$ or $Cu^{\delta+}$ sites. Besides the surface electron polarization, the presence of K also allows the electrons easily polarized upon adsorption of $CO_2$, which occurs to a certain degree at the $O_U{}^{\delta-}$ sites and two $K^{\delta+}$ cations interacted directly with $CO_2$ (see arrows in Figure 6c); yet it is not observed for the $K^{\delta+}$ away from $*CO_2$. Such effect leads to the further stabilization of the molecule on the surface. Given that, our results seem to support the mechanism of molecular polarization and surface electronic polarizability on alkali deposition, which is able to well describe the origin of the observed K-promoted $CO_2$ activation on $Cu_{1.0}O$/Cu(111).

We also notice that $CO_2$ only interacts weakly with $K^{\delta+}$ alone (i.e., physisorption), while the enhanced activity of K/$Cu_{1.0}O$/Cu(111) towards $CO_2$ activation depends on the synergy among $K^{\delta+}$, $O^{\delta-}$ and $Cu^{\delta+}$. $K^{\delta+}$ introduces the surface electron polarization (electronic effect), which enhances the binding between $Cu^{\delta+}$ and C of $CO_2$. As a result, the $O_L$ species on K/$Cu_{1.0}O$/Cu(111) is activated, being able to allow the charge redistribution on $CO_2$ adsorption and therefore the further stabilization of the molecule. $K^{\delta+}$ also participates in the binding directly to stabilize the two terminal oxygen atoms of $CO_2$ (geometric effect). That is, the promotional effect of K heavily relies on the condition that K must be in close proximity of active sites. This is in consistent with the previous study on metal surfaces, showing that alkali-induced reductions in CO dissociation barrier depends strongly on how close K is to the dissociating molecule.[3d]

Overall, our results indicate the selective promoting effect of K deposition on the binding properties of $Cu_xO$/Cu(111) surface, which is only minimal in CO but significant in $CO_2$ activation. It suggests that K cannot alter weak Lewis acid nature of $Cu_xO$/Cu(111), but being able to significantly enhance its Lewis basicity to promote and stabilize the formation of

carbonate species. Our study also shows that the promotion effect of K is complex. The geometric effect alone does not work. The $K^{\delta+}$ sites on $Cu_{1.0}O/Cu(111)$ are not active enough to serve as active sites for catalytic reactions; instead, the combination of electronic and geometric effects is responsible. On one hand, the K deposition leads to the accumulated electron densities over the surface of $Cu_xO/Cu(111)$ (electronic effect); on the other hand, the synergy among $K^{\delta+}$, $O^{\delta-}$ and $Cu^{\delta+}$ assures the enhanced activity towards $CO_2$ activation via direct bonding (geometric effect), or strong polarization/polarizability mechanism (electronic effect). As a result, the promotional effect of K can strongly depends on the concentration and distribution of K in catalysts. It can be easily turned into poison effect if K is over-concentrated.

The observed selective promotion of K in binding properties of metal oxide surface can have a significant impact on the design of catalysts to achieve high activity and selectivity for the complex reactions. In general, a catalyst displays a certain binding properties to the intermediates involved in a catalytic process. Modification of the catalyst using, for instance, dopants is likely to strengthen or weaken the interactions with all the intermediates in similar chemical nature simultaneously.[3j, 28] As a result, a volcano-like correlation is always expected between binding strengths of key intermediates and their catalytic activity.[29] The best catalyst is located at the top of the volcano and usually exhibits a moderate binding, that is, high enough to dissociate reactants and weak enough to allow facile product formation and removal. Further catalyst development is limited by trying to compromise the two criteria operating in an opposite direction. In the present study, the deposition of K not only increases the surface complexity to provide new adsorption sites, but also promotes the activity of other sites on $Cu_xO/Cu(111)$ in a selective way, being able to enhance the Lewis basicity of the surface, but hardly altering weak Lewis acidity. As a result, K deposition only introduces the enhancement the stability of $*CO_2$ and $*CO_3$ rather than *CO on $Cu_xO/Cu(111)$. That is, a modifier, such as K, in some cases can offer new possibilities to "tune" the performance of a catalyst in a way to go beyond the volcano relationship and advance the activity and selectivity via selectively activation to a certain elementary steps involved in a catalytic process. The synergy between the different components can result in a system with a novel performance for catalysis applications.

## 4. Conclusion

We combined STM and DFT to study the promoting effect of K on the atomic and electronic structures as well as chemical activities of $Cu_xO$/Cu(111) ($x \leq 2$). Our results show that K deposition together with the sequential annealing under oxygen atmosphere leads to the further oxidation of $Cu_xO$ film. The deposited K follows a pseudomorphic growth mode and is mainly controlled by strong interaction with chemisorbed O within $O^{\delta-}$-$Cu^{\delta+}$-$O^{\delta-}$ hexagonal ring, which can reach up to 0.19 ML of coverage on $Cu_xO$/Cu(111). In addition, the direct electrostatic interactions, $K^{\delta+}$-$Cu^{\delta+}$ repulsion (3.1~3.5 Å), $K^{\delta+}$-$O^{\delta-}$ attraction (3~4 Å), and $K^{\delta+}$-$K^{\delta+}$ repulsion (5~6 Å), also contribute to control the overall pattern. Our simulated STM images are able to well capture and match the key features of experimental STM images.

The deposition of K displays significant impact on the surface electronic structure of $Cu_xO$/Cu(111). Significant reduction in work function is observed. It leads to a strong electron polarization on the surfaces, which is delocalized not only over $K^{\delta+}$, but also for the entire surface area in a selective way, being able to enhance the Lewis basicity of the surface, but hardly altering weak Lewis acidity. As a result, the promotion of K on the chemical activities of $Cu_xO$/Cu(111) is selective, which varies depending on the nature of adsorbates. The effect is only minimal in CO binding, but significant toward $CO_2$. Our calculations show that the enhancement in $CO_2$ activation depends on the well combination between geometric and electronic effects. On one hand, the K deposition leads to the accumulated electron densities over the surface of $Cu_xO$/Cu(111) (electronic effect), which helps in attracting $CO_2$; on the other hand, the synergy among $K^{\delta+}$, $O^{\delta-}$ and $Cu^{\delta+}$ assures the enhanced activity toward $CO_2$ activation via direct interaction (geometric effect) and strong polarization/polarizibility (electronic effect) mechanisms. To improve the catalytic performance using alkalis, one should be careful to control the concentration and distribution of K in the catalyst. Our results highlight the advantages of using alkalis as promoters in the design of catalysts to achieve high activity and selectivity for the complex reactions.

**Acknowledgment.** The research was carried out at Brookhaven National Laboratory (BNL) under contract DE-SC0012704 with the US Department of Energy, Division of Chemical Sciences. The DFT calculations were performed using computational resources at the Center for Functional Nanomaterials, a US DOE user facility at BNL, the New York Center for Computational Sciences at BNL, and the National Energy Research Scientific Computing Center (NERSC) supported by the Office of Science of the US Department of Energy under Contract No. DE-AC02-05CH11231.

## References


[1] aI. Chorkendorff, H. Niemantsverdriet, *Concepts of Modern Catalysis and Kinetics*, Wiley-VCH, Weinheim, Germany, **2003**; bW. D. Mross, *Catal Rev* **1983**, *25*, 591-637; cM. P. Kiskinova, *Stud. Surf. Sci. Catal.* **1991**, *70*, 1-345.

[2] aG. Ertl, M. Weiss, S. B. Lee, *Chem Phys Lett* **1979**, *60*, 391-394; bA. Politano, G. Chiarello, G. Benedek, E. V. Chulkov, P. M. Echenique, *Surf Sci Rep* **2013**, *68*, 305-389; cA. Politano, V. Formoso, G. Chiarello, *J. Chem. Phys.* **2008**, *129*, 164703-164701-164703-164705; dK. Engvall, L. Holmlid, A. Kotarba, J. B. C. Pettersson, P. G. Menon, P. Skaugset, *Appl Catal a-Gen* **1996**, *134*, 239-246; eA. Kotarba, G. Adamski, Z. Sojka, G. Djega-Mariadassou, *Appl Surf Sci* **2000**, *161*, 105-108; fL. Giordano, G. Pacchioni, *Phys Chem Chem Phys* **2006**, *8*, 3335-3341; gM. Chiesa, E. Giamello, C. Di Valentin, G. Pacchioni, Z. Sojka, S. Van Doorslaer, *J Am Chem Soc* **2005**, *127*, 16935-16944; hA. Kotarba, A. Baranski, S. Hodorowicz, J. Sokolowski, A. Szytula, L. Holmlid, *Catal Lett* **2000**, *67*, 129-134; iM. D. Weisel, J. G. Chen, F. M. Hoffmann, *J Electron Spectrosc* **1990**, *54*, 787-794; jR. L. Toomes, D. A. King, *Surf Sci* **1996**, *349*, 19-42; kF. M. Hoffmann, J. Hrbek, R. A. Depaola, *Chem Phys Lett* **1984**, *106*, 83-86; lF. M. Hoffmann, R. A. Depaola, *Phys Rev Lett* **1984**, *52*, 1697-1700.

[3] aE. Wimmer, S. R. Chubb, C. L. Fu, A. J. Freeman, *J Vac Sci Technol A* **1987**, *5*, 695-696; bJ. J. Mortensen, B. Hammer, J. K. Norskov, *Phys Rev Lett* **1998**, *80*, 4333-4336; cY. Xu, H. Marbach, R. Imbihl, I. G. Kevrekidis, M. Mavrikakis, *J Phys Chem C* **2007**, *111*, 7446-7455; dZ. P. Liu, P. Hu, *J Am Chem Soc* **2001**, *123*, 12596-12604; eJ. C. Park, S. C. Yeo, D. H. Chun, J. T. Lim, J. I. Yang, H. T. Lee, S. Hong, H. M. Lee, C. S. Kim, H. Jung, *J Mater Chem A* **2014**, *2*, 14371-14379; fC. F. Huo, B. S. Wu, P. Gao, Y. Yang, Y. W. Li, H. J. Jiao, *Angew Chem Int Edit* **2011**, *50*, 7403-7406; gS. Stolbov, T. S. Rahman, *Phys Rev Lett* **2006**, *96*; hE. Wimmer, C. L. Fu, A. J. Freeman, *Phys Rev Lett* **1985**, *55*, 2618-2621; iS. J. Jenkins, D. A. King, *J Am Chem Soc* **2000**, *122*, 10610-10614; jC. Liu, P. Liu, *ACS Catalysis* **2015**, *5*, 1004-1012.

[4] J. A. Rodriguez, D. W. Goodman, *Science* **1992**, *257*, 897-903.

[5] aC. S. Chen, W. H. Cheng, S. S. Lin, *Appl Catal a-Gen* **2003**, *238*, 55-67; bJ. A. Rodriguez, J. Graciani, J. Evans, J. B. Park, F. Yang, D. Stacchiola, S. D. Senanayake, S. G. Ma, M. Perez, P. Liu, J. F. Sanz, J. Hrbek, *Angew Chem Int Edit* **2009**, *48*, 8047-8050.

[6] aJ. Graciani, K. Mudiyanselage, F. Xu, A. E. Baber, J. Evans, S. D. Senanayake, D. J. Stacchiola, P. Liu, J. Hrbek, J. F. Sanz, J. A. Rodriguez, *Science* **2014**, *345*, 546-550; bM. Behrens, F. Studt, I. Kasatkin, S. Kuhl, M. Havecker, F. Abild-Pedersen, S. Zander, F. Girgsdies, P. Kurr, B. L. Kniep, M. Tovar, R. W. Fischer, J. K. Norskov, R. Schlogl, *Science* **2012**, *336*, 893-897; cF. M. Hoffmann, K. C. Lin, R. G. Tobin, C. J. Hirschmugl, G. P. Williams, P. Dumas, *Surf Sci* **1992**, *275*, L675-L681; dF. M. Hoffmann, Y. Yang, J. Paul, M. G. White, J. Hrbek, *The Journal of Physical Chemistry Letters* **2010**, *1*, 2130-2134; eR. Schuster, J. V. Barth, G. Ertl, R. J. Behm, *Surf Sci* **1991**, *247*, L229-L234; fR. Schuster, J. V. Barth, J. Wintterlin, R. J. Behm, G. Ertl, *Phys Rev B* **1994**, *50*, 17456-17462; gJ. Onsgaard, L. Thomsen, S. V. Hoffmann, P. J. Godowski, *Vacuum* **2006**, *81*, 25-31; hJ. Onsgaard, L. Bech, C. Svensgaard, P. J. Godowski, S. V. Hoffmann, *Prog Surf Sci* **2001**, *67*, 205-216; iJ. Onsgaard, S. V. Hoffmann, P. J. Godowski, P. Moller, J. B. Wagner, A. Groso, A. Baraldi, G. Comelli, G. Paolucci, *Chem Phys Lett*

**2000**, *322*, 247-254; jL. Bech, J. Onsgaard, S. V. Hoffmann, P. J. Godowski, *Surf Sci* **2001**, *482*, 243-249; kJ. Onsgaard, S. V. Hoffmann, P. Moller, P. J. Godowski, J. B. Wagner, G. Paolucci, A. Baraldi, G. Comelli, A. Groso, *Chemphyschem* **2003**, *4*, 466-473.

[7] R. Xu, S. H. Zhang, C. B. Roberts, *Ind Eng Chem Res* **2013**, *52*, 14514-14524.

[8] aF. Yang, J. Graciani, J. Evans, P. Liu, J. Hrbek, J. F. Sanz, J. A. Rodriguez, *J Am Chem Soc* **2011**, *133*, 3444-3451; bB. White, M. Yin, A. Hall, D. Le, S. Stolbov, T. Rahman, N. Turro, S. O'Brien, *Nano Lett* **2006**, *6*, 2095-2098; cA. E. Baber, X. F. Yang, H. Y. Kim, K. Mudiyanselage, M. Soldemo, J. Weissenrieder, S. D. Senanayake, A. Al-Mahboob, J. T. Sadowski, J. Evans, J. A. Rodriguez, P. Liu, F. M. Hoffmann, J. G. G. Chen, D. J. Stacchiola, *Angew Chem Int Edit* **2014**, *53*, 5336-5340.

[9] G. Ertl, *Surf Sci* **1967**, *6*, 208-232.

[10] J. C. Hanson, R. Si, W. Xu, S. D. Senanayake, K. Mudiyanselage, D. Stacchiola, J. A. Rodriguez, H. Zhao, K. A. Beyer, G. Jennings, K. W. Chapman, P. J. Chupas, A. Martínez-Arias, *Catalysis Today* **2014**, *229*, 64-71.

[11] aF. Jensen, F. Besenbacher, I. Stensgaard, *Surf Sci* **1992**, *270*, 400-404; bF. Jensen, F. Besenbacher, E. Laegsgaard, I. Stensgaard, *Surf Sci* **1991**, *259*, L774-L780.

[12] T. Matsumoto, R. A. Bennett, P. Stone, T. Yamada, K. Domen, M. Bowker, *Surf Sci* **2001**, *471*, 225-245.

[13] aF. Yang, Y. Choi, P. Liu, D. Stacchiola, J. Hrbek, J. A. Rodriguez, *J Am Chem Soc* **2011**, *133*, 11474-11477; bF. Yang, Y. Choi, P. Liu, J. Hrbek, J. A. Rodriguez, *J Phys Chem C* **2010**, *114*, 17042-17050; cK. Mudiyanselage, A. Wei, F. Yang, P. Liu, J. D. Stacchiola, *Phys Chem Chem Phys* **2013**, *15*, 10726-10731.

[14] aG. Kresse, J. Hafner, *Phys. Rev. B* **1993**, *47*, 558-561; bG. Kresse, J. Furthmuller, *Phys. Rev. B* **1996**, *54*, 11169-11186.

[15] aP. E. Blochl, *Phys. Rev. B* **1994**, *50*, 17953-17979; bG. Kresse, D. Joubert, *Phys. Rev. B* **1999**, *59*, 1758-1775.

[16] aJ. P. Perdew, J. A. Chevary, S. H. Vosko, K. A. Jackson, M. R. Pederson, D. J. Singh, C. Fiolhais, *Phys. Rev. B* **1992**, *46*, 6671-6687; bJ. P. Perdew, J. A. Chevary, S. H. Vosko, K. A. Jackson, M. R. Pederson, D. J. Singh, C. Fiolhais, *Phys Rev B* **1993**, *48*, 4978-4978.

[17] A. Soon, M. Todorova, B. Delley, C. Stampfl, *Phys Rev B* **2006**, *73*.

[18] H. J. Monkhorst, J. D. Pack, *Phys Rev B* **1976**, *13*, 5188-5192.

[19] D. Torres, N. Lopez, F. Illas, R. M. Lambert, *Angewandte Chemie* **2007**, *119*, 2101-2104.

[20] W. An, A. E. Baber, F. Xu, M. Soldemo, J. Weissenrieder, D. Stacchiola, P. Liu, *ChemCatChem* **2014**, *6*, 2364-2372.

[21] A. Zangwill, *Physics at Surface*, Cambridge University Press, Cambridge, **1988**.

[22] W. Zhao, G. Kerner, M. Asscher, X. M. Wilde, K. Al-Shamery, H. J. Freund, V. Staemmler, M. Wieszbowska, *Phys Rev B* **2000**, *62*, 7527-7534.

[23] U. Martinez, L. Giordano, G. Pacchioni, *The Journal of Chemical Physics* **2008**, *128*, 164707.

[24] aJ. A. Rodriguez, P. Liu, J. F. Viñes, F. Illas, Y. Takahashi, K. Nakamura, *Angew. Chemi. Int. Ed.* **2008**, *47*, 6685-6689; bJ. A. Rodriguez, P. Liu, Y. Takahashi, K. Nakamura, F. Viñes, F. Illas, *J Am Chem Soc* **2009**, *131*, 8595-8602.

[25] S. D. Jackson, J. S. J. Hargreaves, Willey-VCH Verlag GmbH, Weinheim, **2008**.

[26] D. Martin, D. Duprez, *J Mol Catal a-Chem* **1997**, *118*, 113-128.

[27] J. A. Rodriguez, J. Evans, L. Feria, A. B. Vidal, P. Liu, K. Nakamura, F. Illas, *Journal of Catalysis* **2013**, *307*, 162-169.
[28] aY. Yang, M. G. White, P. Liu, *The Journal of Physical Chemistry C* **2012**, *116*, 248-256; bM. Behrens, F. Studt, I. Kasatkin, S. Kühl, M. Hävecker, F. Abild-Pedersen, S. Zander, F. Girgsdies, P. Kurr, B.-L. Kniep, M. Tovar, R. W. Fischer, J. K. Nørskov, R. Schlögl, *Science* **2012**, *336*, 893-897.
[29] aP. Liu, Y. Yang, M. G. White, *Surf Sci Rep* **2013**, *68*, 233-272; bJ. K. Norskov, T. Bligaard, J. Rossmeisl, C. H. Christensen, *Nat Chem* **2009**, *1*, 37-46.

**Captions**

Figure 1. (a,b) Optimized $Cu_{1.1}O/Cu(111)$ surface structure with 0.50 ML of oxygen coverage to model the 44- or 29-structures. The unit cells for 44-structure (10.8Å × 20.6 Å 77.8°, a) and 29-structure (7.9Å × 17.8 78.1°, b) were outlined in blue of against experiment (green-line). Black ball: chemisorbed $O(O_{ad})$. (c) Experimental STM image of 44-structure scanned at room temperature: 0.45 nA, 1.24V, 44 unit cell of (11.2 ± 0.1Å) × (21.9 ± 0.1 Å) 76.4° is highlighted; (d) Experimental STM image of 29-structure scanned at room temperature: 0.49nA; 1.10V, 29 unit cell of (9.2 ± 0.1Å) × (18.0 ± 0.1 Å) 84.9° was highlighted. $O_{ad}$ was not labeled in (c) and (d).

Figure 2. (a) Experimental STM image of K-deposited $Cu_xO/Cu(111)$ scanned at room temperature which was followed by a sequential annealing in $5\times10^{-7}$ Torr $O_2$ at 500 K for 10 min: 0.87 nA, 1.68 V. The arrow vectors denoted four unit cells. The inset: an 20 × 20 $nm^2$ STM image of K-deposited $Cu_xO/Cu(111)$ surface prepared by room temperature deposition: 0.52 nA, 0.49 V. (b) DFT-optimized structure for 0.19 ML of K deposited on the $Cu_{1.1}O/Cu(111)$, where the corresponding simulated STM image with constant current mode at -1.2 V sample bias was shown in (c)**.** Red: O; Brown: Cu; Purple: K.

Figure 3. (a) Calculated PDOS of various O 2p before (red) and after (blue) 0.19 ML K deposition on $Cu_{1.1}O/Cu(111)$. Top: $O_U$; middle: $O_L$; bottom: $O_{chem}$. (b) Calculated PDOS of Cu 3d on $Cu_{1.1}O/Cu(111)$ before (red) and after (blue) K-deposition, as well as comparison of $K^{\delta+}$ and $O^{\delta+}$ PDOS with those of $K_2O$.

Figure 4. Calculated ELF (electron localization function) of the $Cu_{1.1}O/Cu(111)$ before (a) and after (b) the deposition of 0.19 ML K, where the projected 2D slices over and normal to the surface are displayed. Color scheme: blue, purple, and red balls represent Cu, K, and O atoms, respectively. The isosurface level was chosen as $0.3e/a_0^3$ ($a_0$ = Bohr radius).

Figure 5. Optimized structures for CO (a), $CO_2$ (b) and $CO_2$ (c) adsorption on 0.19 ML K deposition on $Cu_{1.1}O/Cu(111)$. Binding energy on $Cu_{1.1}O/Cu(111)$ were included for comparison. Red: O; Brown: Cu; Purple: K; Grey: C.

Figure 6. Calculated charge density difference $\Delta\rho$, $\Delta\rho = \rho_{(slab+ads)} - \rho_{slab} - \rho_{ads}$ with ads=CO or $CO_2$, for CO and $CO_2$ adsorbed on 0.19 ML K deposition on $Cu_{1.0}O/Cu(111)$ shown in Figure 5a and 5b. (a) CO adsorption: side view, (b) CO adsorption: top view, (c) $CO_2$ adsorption: side view, (b) $CO_2$ adsorption: top view. The isosurface level was chosen as $0.001\ e/a_0^3$ ($a_0$ = Bohr radius). Yellow and cyan isosurfaces represent charge accumulation (i.e., gain of electron density) and depletion (i.e., loss of electron density) in the space, respectively. Blue: Cu; Red: O; Purple: K; Grey: C.

**Figures**

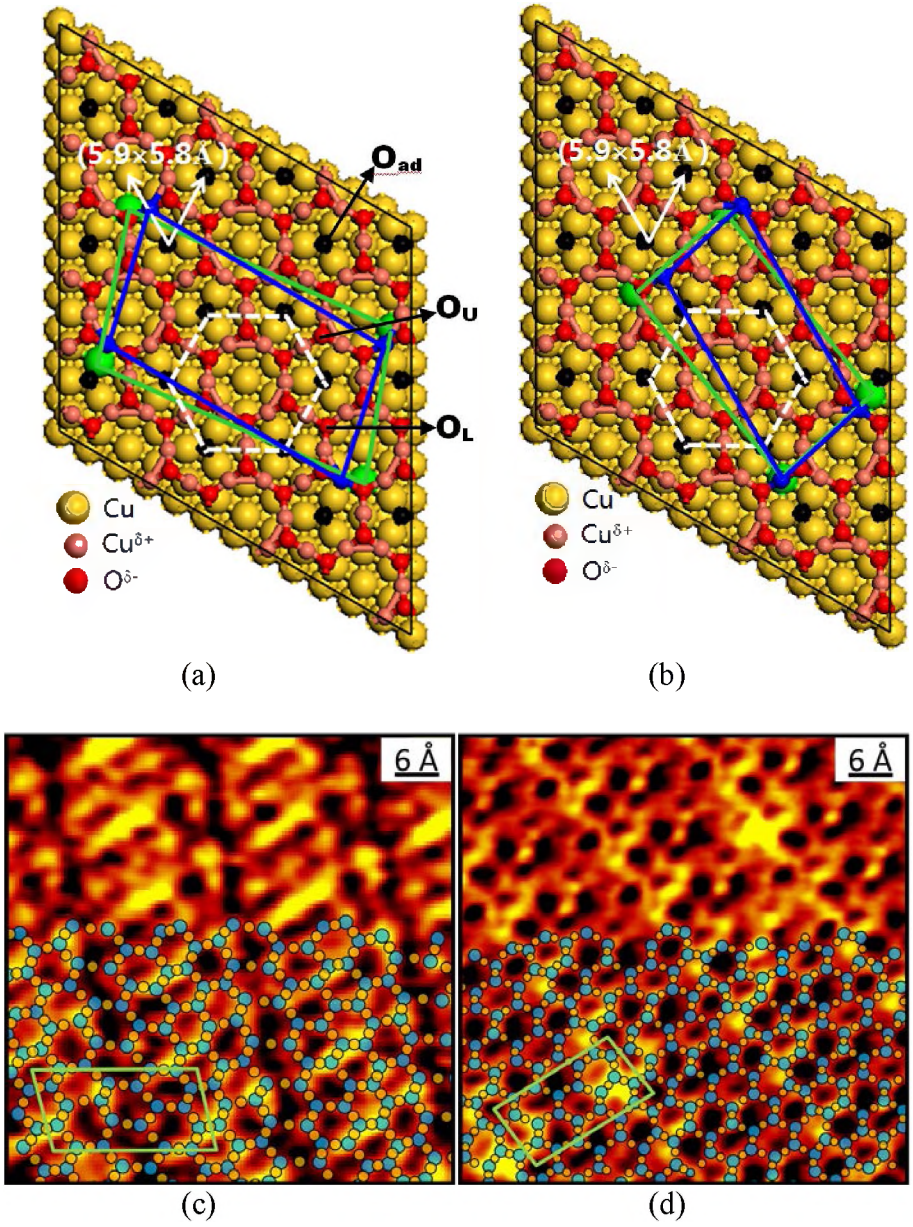


Figure 1.

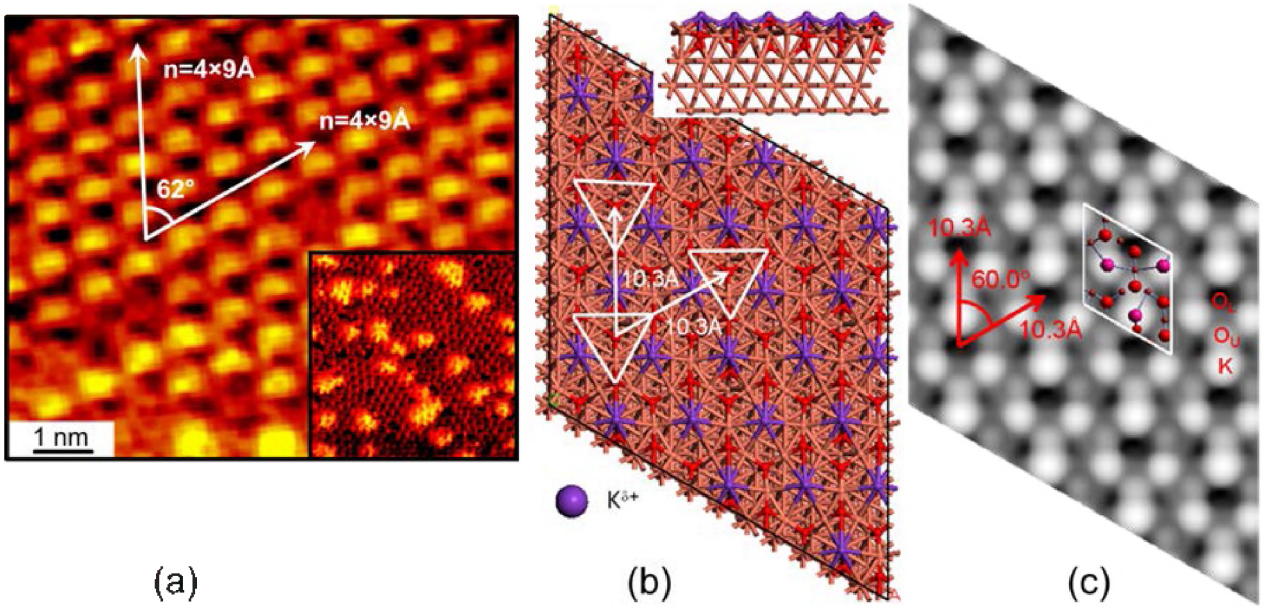


Figure 2.

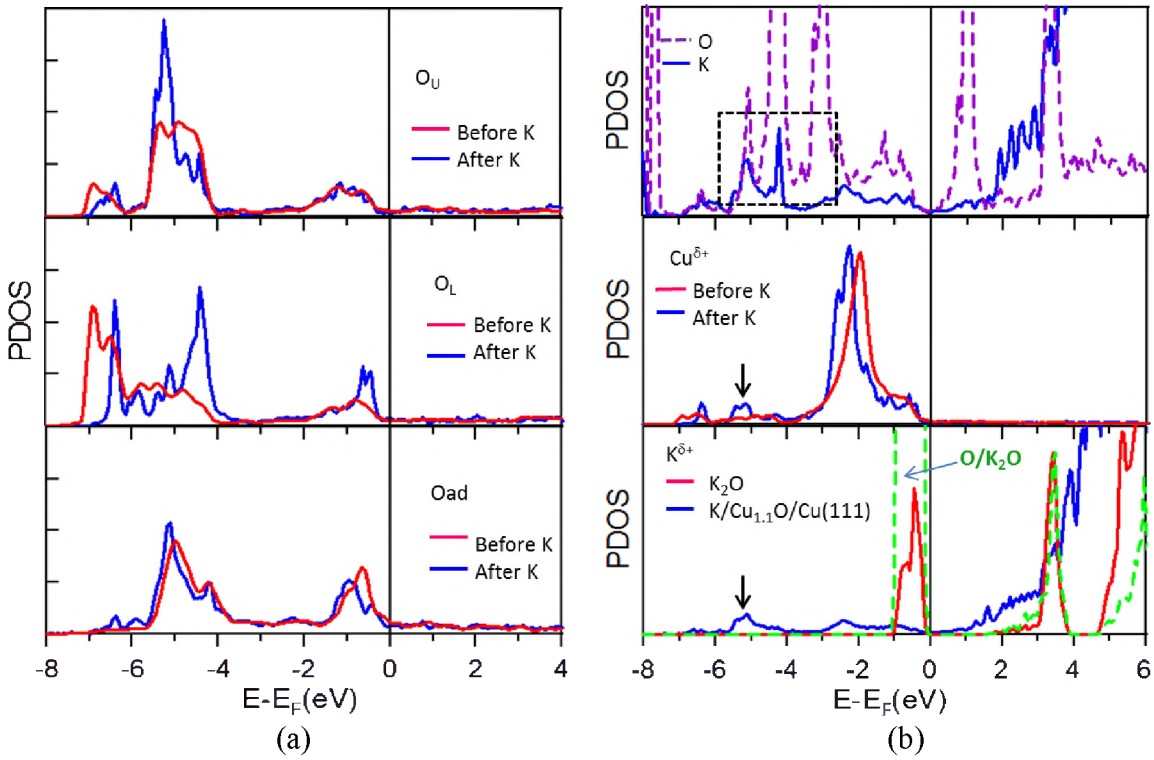
PDOS
$O_U$
Before K
After K
$O_L$
Before K
After K
Oad
Before K
After K
-8 -6 -4 -2 0 2 4
E-E$_F$(eV)
(a)
PDOS
O
K
$Cu^{\delta+}$
Before K
After K
$K^{\delta+}$
$K_2O$
K/$Cu_{1.1}$O/Cu(111)
O/$K_2O$
-8 -6 -4 -2 0 2 4 6
E-E$_F$(eV)
(b)

Figure 3.

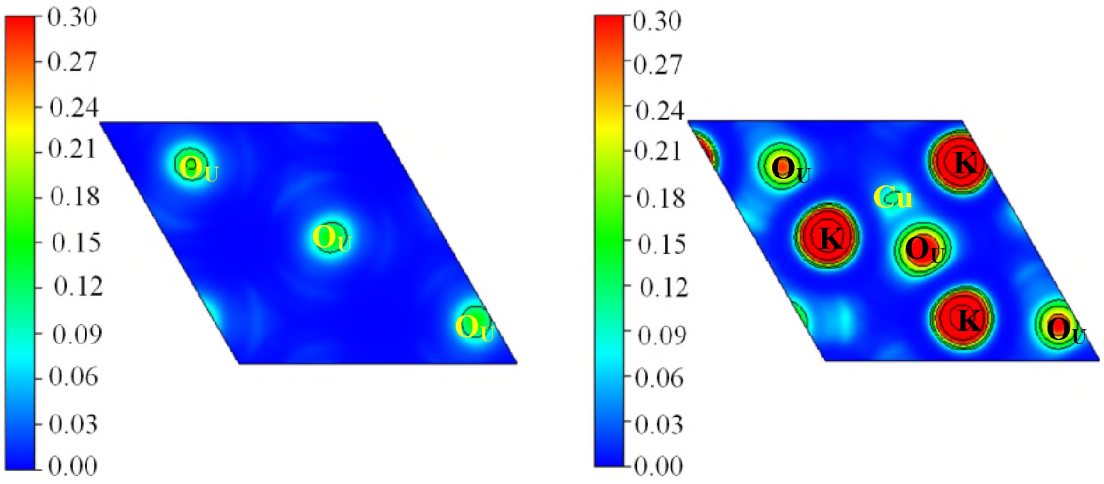
0.30
0.27
0.24
0.21
0.18
0.15
0.12
0.09
0.06
0.03
0.00
O
O
O
(a)
0.30
0.27
0.24
0.21
0.18
0.15
0.12
0.09
0.06
0.03
0.00
O
K
Cu
K
O
K
O
(b)

Figure 4.

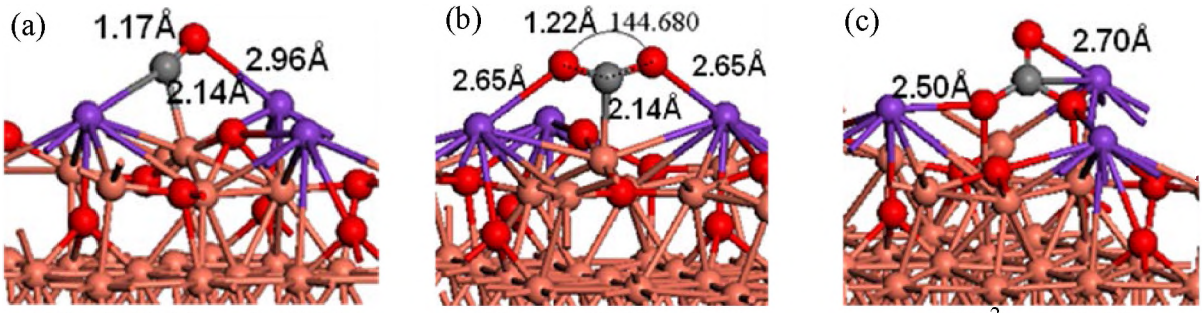


CO: -0.49eV *vs* -0.47eV $CO_2$: -0.48eV *vs* 0eV $CO_3^{2-}$: -1.41eV

Figure 5.

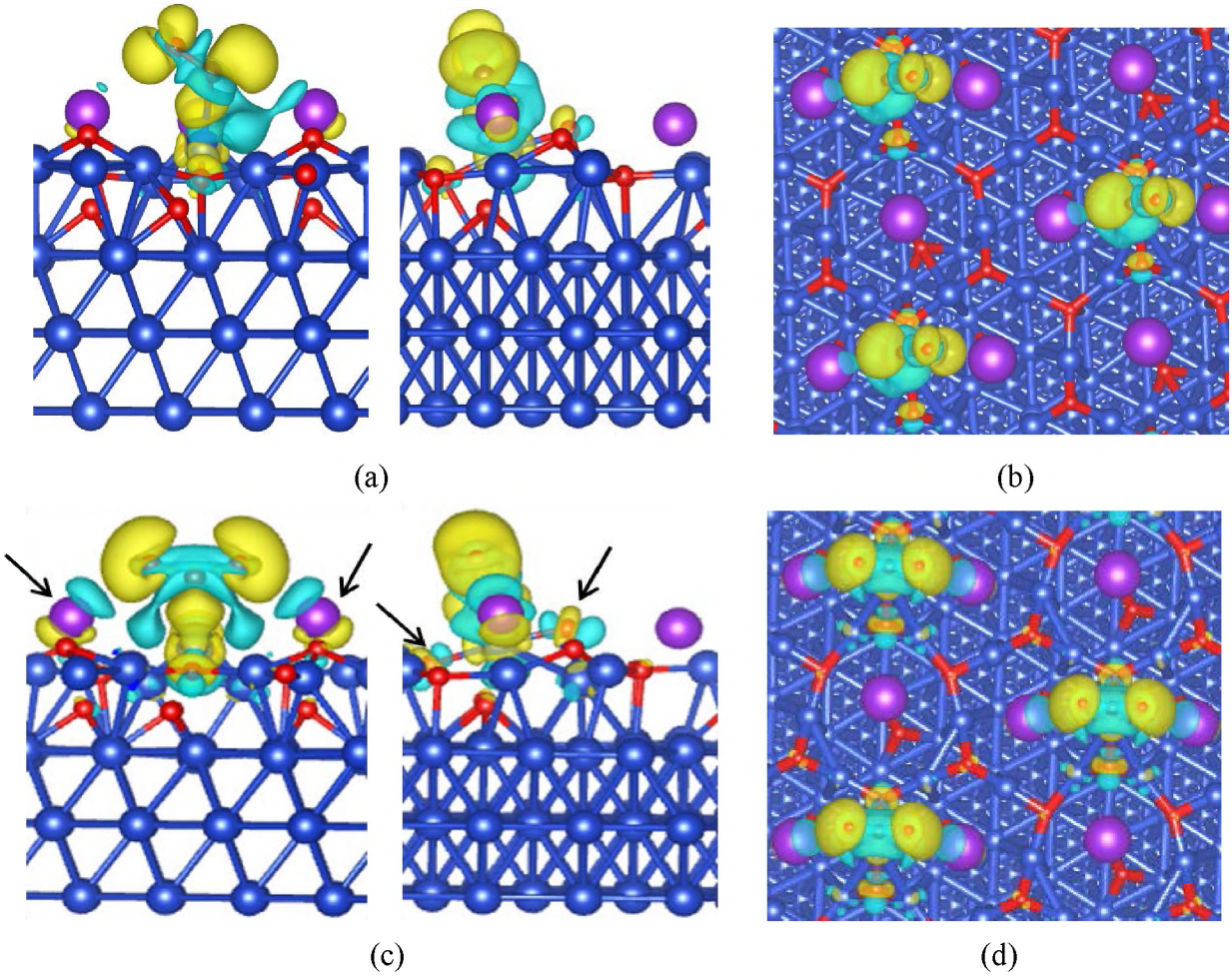


Figure 6.

**TOC**